Multi-Vector Boson Production via Gluon-Gluon Fusion

Pankaj Agrawal and Ambresh Shivaji
Institute of Physics
Sachivalaya Marg
Bhubaneswar 751005, INDIA

The data is being recorded at the Large Hadron Collider (LHC) for quite sometime. All this data has produced only strong support for the standard model (SM). There does not seem to be any significant evidence for beyond the standard model (BSM) scenarios [**?**]. Various extensions of the SM are getting seriously constrained. There also appear to be strong suggestions that the only missing piece of the SM, the Higgs boson exists. However, the SM is unsatisfactory in a number of ways. One has to keep looking for any hint of the new physics signal. It would appear that to test the model and look for the directions for the extension, one may need to probe as many SM processes as possible. In particular, one would be looking for the processes that have many particles in the final state or have small cross sections.

At the LHC and proposed hadron colliders such as HE-LHC, one of the features is large gluon luminosity. Therefore, some of the gg scattering processes, which occur at the one-loop level and have many particles in the final state, would be important and observable at the LHC. They can also contribute to the backgrounds to the BSM physics scenarios. We are interested in a particular set of processes $pp \to VV'g/\gamma X$. Here $V, V' = W, Z, \gamma$. We are particularly interested in the contribution from the gluon-gluon scattering. Since W, Z, γ do not couple to the gluons directly, these processes take place at the one-loop.

A selection of the processes of interest are:

$$gg \to \gamma\gamma g,\ \gamma Z g,\ \gamma Z\gamma, \tag{1}$$
$$gg \to ZZg,\ ZZ\gamma,\ ZZZ, \tag{2}$$
$$gg \to WWg,\ WW\gamma,\ WWZ. \tag{3}$$

The process $gg \to \gamma\gamma g$ has already been examined long ago. Our primary focus would be on the process $gg \to \gamma Z g$, with some comments on the other processes. The work on some of these processes has been reported in [**?**]. These processes occur at one-loop. The one-loop diagrams that make contribution are box-type and pentagon-type diagrams. For the processes involving W-bosons, there are also triangle-type diagrams. These diagrams have a quark loop. We have also considered the possibility of a heavy quark in the loop, i.e., the top quark. For the processes (1), for each

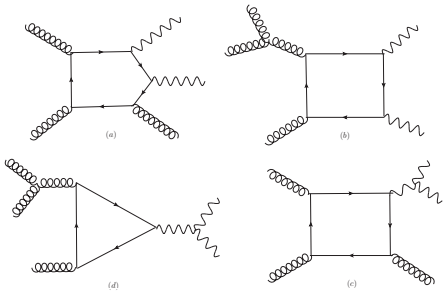

Figure 1: Typical diagrams contributing to the processes.

quark flavour, there are 24 pentagon-type and 18 box-type diagrams. Only half of these diagrams are independent. Because of the Z-boson, the amplitude of both box-type and pentagon-type diagrams is sum of vector coupling and axial-vector coupling parts. In the case of box-type diagrams, the axial-vector coupling pieces add up to zero (Furry's theorem). So the box-type diagrams contribute only through vector coupling of the Z-boson. The process $gg \to \gamma Z\gamma$ gets contribution from only pentagon-type diagrams. Furthermore, here vector coupling contributions add up to zero. So there is contribution from axial-vector couping of the Z-boson only.

Details of our calculation can be found in [**?**, **?**]. For each class of diagrams, we write down the amplitude for a prototype diagram. The amplitude for the rest of the diagrams is generated by appropriate permutations of the external legs. One has to be a bit careful due the presence of γ_5 in the amplitude. The trace of γ matrices is computed in d dimensions using FORM. The amplitude is now written in terms of tensor integrals. The most complicated tensor integral that appears in the calculations is:

$$E^{\mu\nu\rho\sigma\delta} = \int \frac{d^dk}{(2\pi)^d} \frac{k^\mu k^\nu k^\rho k^\sigma k^\delta}{N_0 N_1 N_2 N_3 N_4} \,. \tag{4}$$

Here, $N_i = k_i^2 - m_q^2 + i\epsilon$ and k_i is the momentum of the i^{th} internal line in the corresponding scalar integrals; $d = (4 - 2\epsilon)$ and m_q is the mass of the quark in the loop. We also examine the effect of non-zero m_q.

The tensor integrals are reduced to scalar integrals using the techniques of Oldenborgh and Vermaseren. For massless quarks in the loop, we have computed the scalar integrals and checked with existing results. For the massive quarks in the loop, we use OneLOop library for the bubble, triangle, and box scalar integrals. For the pentagon scalar integrals, we use the result of vanNeerven. One can write pentagon scalar integral in terms of box scalar integrals, $E_0 = \sum_{i=0}^{4} c_i D_0^{(i)}$.

We have made a number of checks on our calculation. The process is UV finite.

Pentagram diagrams are obviously UV finite. But individual box diagram is not. However, when we add box diagrams, the UV divergences cancel. We have checked that the mass singularities which show up as $\log^2(\mathrm{m_q})$ and $\log(\mathrm{m_q})$ also cancel. There is no soft IR divergence, as we will be making p_T cuts on the jets. We have checked the gauge invariance by replacing the polarization vector of $g/\gamma/Z$ bosons with the corresponding momentum vector. The amplitude vanishes when we make this replacement for the photon, gluon and suitably for the Z-boson.

We compute the amplitude numerically. To do the phase space integration, we use a PVM implementation of the VEGAS algorithm (AMCI) and run the code on a cluster of machines. In Fig 2(i), we display cross section as a function of centre-of-mass (CM) energy. These results include following kinematic cuts: $P_T^{\gamma,Z,j} > 50$ GeV, $|\eta^{\gamma,\mathrm{Z,j}}| < 2.5,\ \mathrm{R}(\gamma,\mathrm{j}) > 0.6$. We have also chosen factorization and renormalization scales as $\mu_f = \mu_R = p_T^Z$. Rest of the results are for the CM energy of 14 TeV. In Fig 2(ii), we show the cross section as a function of p_T^{min}. Fig 3 displays the p_T and η distributions for the gluon-jet and the photon. The plots for the Z-boson are similar to that of the photon. We observe that few hundred such events have already been produced at the LHC by now. Of course, one will have to dig it out of other tree-level processes with the identical final state. We note that the photon p_T distribution is harder, as compared to the gluon-jet distribution. It is because the photon is emitted from the quark loop, while the gluon can be emitted from another gluon (in the box diagram). The rapidity distribution of the gluon-jet is also more spread out. The virtue of this is that a cut on p_T and rapidity of a photon can be used to discriminate from the processes where it is emitted directly as bremsstrahlung, like in quark initiated processes. We find that the top-quark makes negligible contribution to the process. This decoupling of a quark occurs starting around $m_q = 100$ GeV.

The results for the process $gg \to \gamma\gamma g$ are already in literature for massless quark in the loop. We included heavy-quark, top-quark, in the calculation and found that it made negligible contribution. The typical cross-section for $p_T^{min} = 30$ GeV, at 14 TeV LHC, is about 642 fb. The cross-section for the process $gg \to \gamma\gamma Z$ is quite small, as expected. It is about 0.05 fb.

In conclusion, we have presented brief results for the processes $gg \to \gamma Z g, \gamma Z \gamma$. These are standard model processes and cross sections are large enough so that these processes could be observable at the LHC. More detailed results can be found in [**?**, **?**].

References

[1] G. Rolandi, "LHC Results - Highlights," Arxiv:1211.3718 [hep-ex]

[2] P. Agrawal and A. Shivaji, Phys. Rev. D**86**, 073013 (2012) and references therein.

[3] P. Agrawal and A. Shivaji, Arxiv:1208.2593 [hep-ph] and references therein.

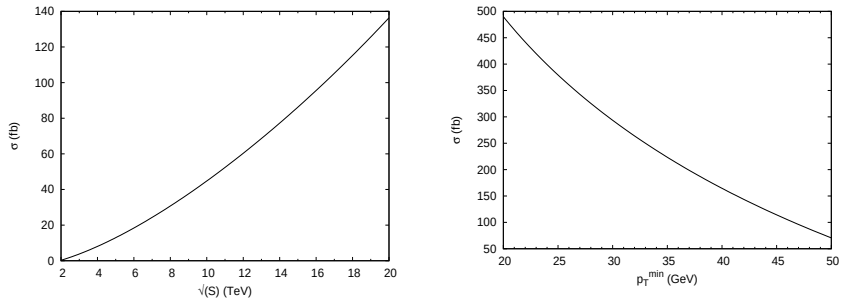

(i) (ii)

Figure 2: (i) Centre of mass energy (ii) p_T^{min} dependence (at 14 TeV) of the cross section for $gg \to \gamma Z g$.

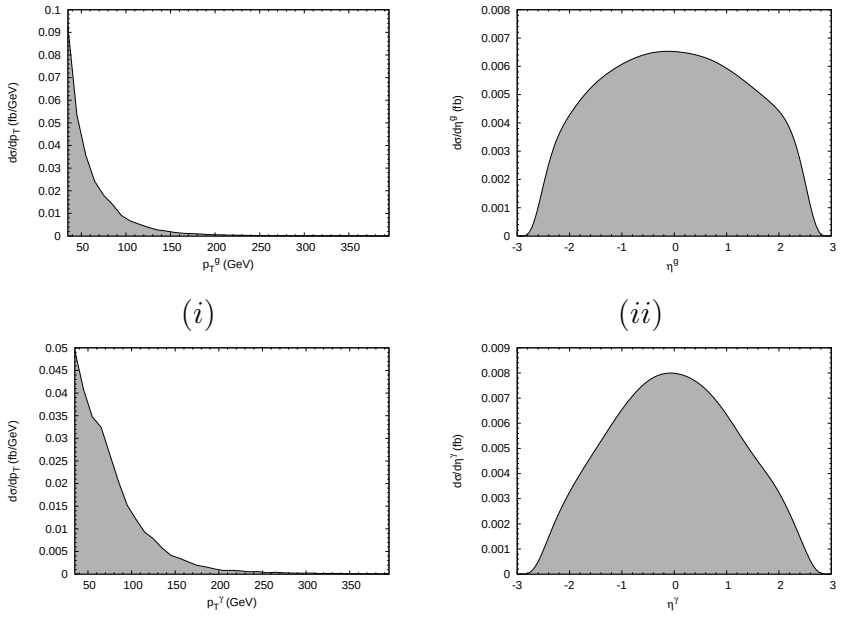

(i) (ii)

(iii) (iv)

Figure 3: (i) p_T and (ii) η distributions of the gluon; (iii) p_T and (iv) η distributions of the photon.